ISSN 1996-5044

Research Journal of

Nanoscience and Nanotechnology

http://knowledgiascientific.com

Knowledgia SCIENTIFIC
A Place to Publish Outstanding Research

Research Journal of Nanoscience and Nanotechnology 2 (1): 24-30, 2012
ISSN 1996-5044 / DOI: 10.3923/rjnn.2012.24.30

Pulsed Laser Deposition of TTB-type Materials Thin Films Examples of $Pb_2KNb_5O_{15}$ (PKN) and $GdK_2Nb_5O_{15}$ (GKN)

[1]Y. Gagou, [2]A. Menny, [1]J. Belhadi, [3]M.A. Fremy, [4]D. Mezzane, [1]Y. Baledent, [5]K. Djellab, [1]M. El Marssi and [6,7]P. Saint-Gregoire

[1]LPMC, Université de Picardie Jules Verne, 33 rue saint Leu, 80039 Amiens Cedex, France
[2]FST, Université de Nouakchott, B.P 5026, Nouakchott, Mauritanie
[3]IM2NP, Université du Sud Toulon Var, Ave. de l' Univ., BP 20132, 83957 La Garde cedex, France
[4]LMCN, FSTG, University Cadi Ayyad Marrakech, Morocco
[5]LRCS, Université de Picardie Jules Verne, 33 rue saint Leu, 80039 Amiens Cedex, France
[6]University of Nîmes, Laboratory MIPA, Department of Sciences and Arts, 30021 NIMES cedex 01,
[7]ICGM (UMR CNRS n°5253), C2M, 34095 Montpellier cedex, France

Corresponding Author: P. Saint-Gregoire, University of Nimes, Laboratory MIPA, 30021 NIMES Cedex 01, France

ABSTRACT

$Pb_2KNb_5O_{15}$ (PKN) and $GdK_2Nb_5O_{15}$ (GKN) thin films were elaborated by Pulsed Laser Deposition (PLD) technique on (100)MgO coated $LaSr_{0.5}Co_{0.5}O_3$ (LSC/MgO) and on (100) MgO coated $SrRuO_3$ (SRO/MgO) substrates. The quality of films was controlled by X-ray diffraction and Reflection High Energy Electron Diffraction (RHEED) and shown to be good. Films grow with the crystallographic c axis perpendicular to the layer. This result is important because it opens the possibility to obtain films of TTB compounds with a controlled modulation of composition in the c-direction and as a consequence with tailored physical properties.

Key words: Thin film, ferroelectric, TTB, PLD, oxides

INTRODUCTION

The ferroelectric niobates of Tetragonal Tungsten Bronze (TTB) type are attractive materials for their dielectric, ferroelectric, photorefractive, pyroelectric and piezoelectric properties (Zhang *et al.*, 1996; Vre and Hesselink, 1994; Aronson and Hesselink, 1990). Built on a network of XO6 octahedra sharing corners (in our case X = Nb), the structure presents cavities forming tunnels along the crystallographic axis c. Filling of these empty spaces in the TTB structure by various cations, provides a rich phase diagram constituted by a series of intermediate phases and a diffusive ferroelectric phase transition with enhanced dielectric and piezoelectric constants (Hesselink and Bashaw, 1993; Sakamoto and Yazaki, 1973) and hence governs strongly the physical properties. Since these compounds are used for a wide variety of applications in electronic, electro-optic, optical, acoustic devices likeholographic data storages, spatial light modulators, pyroelectric sensors, Surface Acoustic Wave (SAW) devices and beam steering (Webster and Zernike, 1976; Castellans and Feinstein, 1979) where miniaturization is a challenge, it is important to master the elaboration of thin films. Moreover, since the physical properties of these materials are strongly governed by the presence of cations in the tunnels,

the perspective of changing in a film, the composition along tunnels, is a challenge that would lead to the possibility of tailoring properties. In that respect, the present work describing the elaboration of films with different compositions is a first step in the direction of future elaborations of epitaxial multilayers with different compositions.

The Pulsed Laser Deposition (PLD) is a suitable thin-film deposition technique for the preparation of epitaxial oxide films on different substrates, with an optimal control that can well compete with other methods as Molecular Beam Epitaxy (MBE) (Mohammadkhani *et al.*, 2010). The choice of the substrate was mainly defined by the search to minimize the mismatch between its structure and that of the film. Taking into account the structure of the compounds deposited in this work, it was expected that layers would likely grow perpendicular to the crystallographic axis c; hence, the two single-crystal substrates (100) MgO and (100) STO appeared to present favourable cases to obtain epitaxial layers in reason of the value of crystalline parameters, a situation that could be favourable to the use of these materials in ferroelectric FeRAMs (Tse and Chan, 2003). The (100) MgO was coated with $LaSr_{0.5}Co_{0.5}O_3$ (hereafter noted LSC/MgO) and with $SrRuO_3$ (hereafter noted SRO/MgO) in order to improve the fit between crystalline parameters.

EXPERIMENTAL CONDITIONS

Using Pulsed Laser Deposition technique (PLD), we have grown lead potassium niobate $Pb_2KNb_5O_{15}$ (PKN) and $GdK_2Nb_5O_{15}$ (GKN) thin films from dense ceramic targets. The targets were obtained by solid state reaction between oxides (PbO or Gd_2O_3 and Nb_2O_5) and carbonate (K_2CO_3) in appropriate sintering treatment. A Lambda-Physik EMG 103 KrF excimer laser with e = 248 nm, operating with various pulse repetition rates was used for the films growth. The Laser pulses were focused on the rotating targets as a spot having a 2 mm^2 surface which corresponds to laser fluency of 2-3 J cm^{-2}. The final frequency of laser pulses was 3 Hz. The Meca2000 deposition chamber is equipped with a furnace especially designed to heat substrates up to temperatures as high as 900°C to achieve a good crystallization. The thin films have been deposited in an oxygen partial pressure in the range of 0.2-0.3 mbar, with a substrate temperature range of 720-750°C. However, the epitaxial control of thin films is complex and parameters like deposition time (or total number of pulse), distance between the target and the substrate, were studied and then selected to obtain the formation of a well oriented crystalline TTB structure. The PLD system is also equipped with Reflection High Energy Electron Diffraction (RHEED) technique for the film surface characterization. The thickness of the PKN films ranges between 90 and 300 nm and could be calculated by the total number of pulses and Laue oscillations calculated values. The crystalline phase of the thin film was characterized by X-ray Diffraction (XRD) measurements using a Siemens D5000 classical diffractometer.

RESULTS

X-ray characterisation of targets: The diffraction pattern of the GKN target is presented in Fig. 1, where we can observe the most intense line located around $2\theta \approx 32°$ for the annealed target, characteristic of the TTB structure. It shows that the GKN target is well crystallized and lattice parameters have been refined from X-ray pattern by Rietveld method using Fullprof (Rodriguez-Carvajal, 1993). In this Fig. 1, we also present the result of refined structure in P4 bm space group showing the observed and the calculated diagrams and their difference. The lattice parameters obtained from profile adjustment, are: A = b = 12.429 Å and c = 3.896 Å, with a reliability factor $\chi^2 = 1.28$ obtained in a rapid convergent calculation.

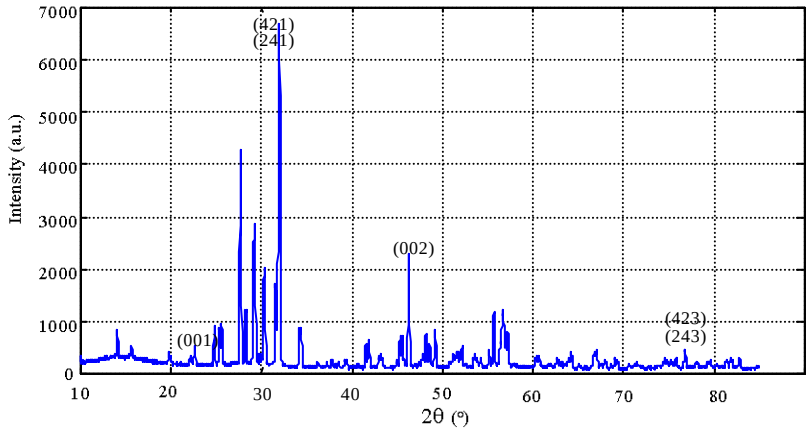

Fig. 1: Refined diagram of GKN ceramic using Fullprof, showing observed and calculated intensities and their difference

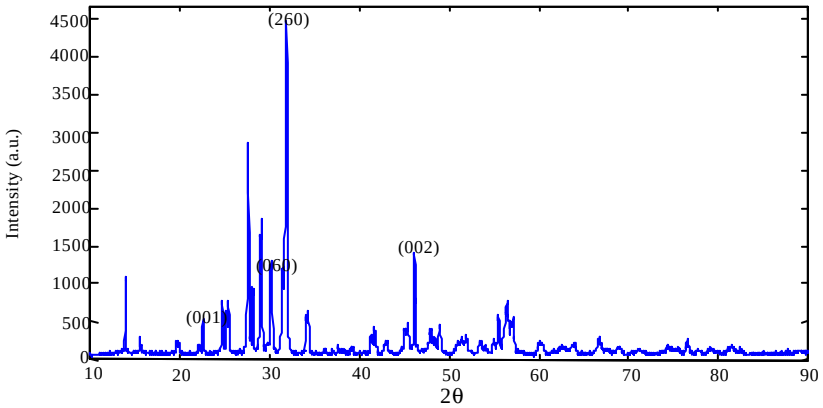

Fig. 2: X-ray diagram from PKN ceramic which serves as PLD target

The X-ray diffraction pattern recorded on PKN targets is shown in Fig. 2. This diagram that evidences also the good crystalline character of the target, was refined and indexed in the TTB orthorhombic structure with a =17.59 Å, b =17.83 Å and c = 3.97 Å, in good agreement with reported values (Kimura *et al.*, 2005).

X-ray study of thin films: X-ray diffraction diagrams presented in Fig. 3 show a structural orientation with the GKN c-axis direction perpendicular to the substrate. A single TTB crystalline phase was observed after the elaborated thin film annealing at 900°C during 4 h. The good quality of the thin film was proved by the full width at half maximum (FWHM) calculated on the GKN (001) line. Its value is about 2.34° and can be optimized by several annealings. The recorded rocking curve is presented in the inset of Fig. 3.

The thickness of the thin film is about 5000 Å (estimated from the deposition rate of GKN). As shown in Fig. 3, only (00l) lines orientations were indexed in GKN structure in the X-ray diffraction pattern.

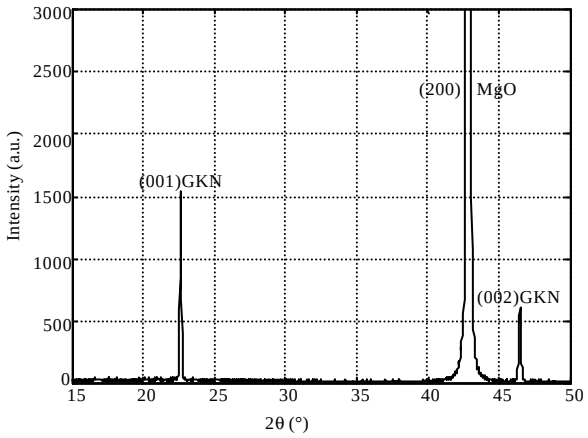

Fig. 3: X-ray pattern of GKN thin film grown on SRO/(100)MgO substrate

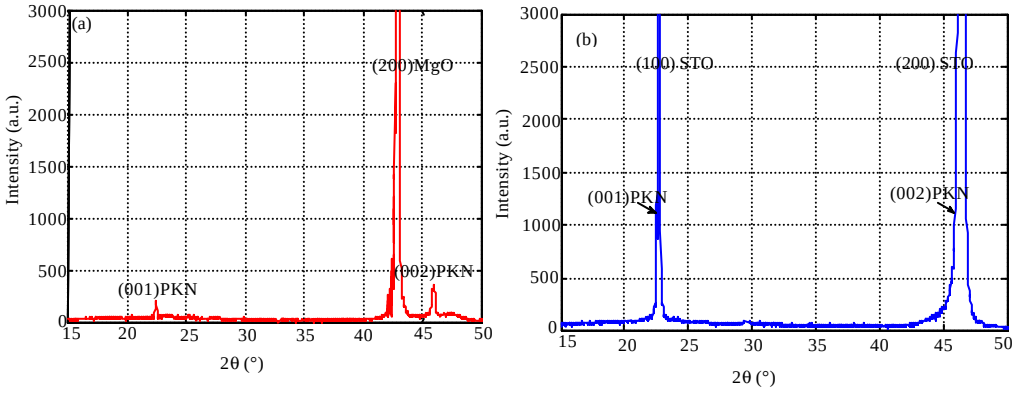

Fig. 4(a-b): X-ray diffraction pattern from PKN thin film grown on MgO (a) and STO (b) substrates

The diffraction pattern of elaborated PKN thin films is presented in Fig. 4. Figure 4a presents the pattern obtained with a thin film of PKN on MgO substrate, whereas Fig. 4b corresponds to a PKN thin film deposited on STO.

To highlight the influence of the substrate on the epitaxial growth of the film, another PKN thin film was indeed elaborated, using a $SrTiO_3$ (STO) substrate; optimal experimental growth conditions appear to be close to those used with the former substrate: pressure of 0.25 mbar, substrate temperature of 740°C and distance between target and substrate of 3 cm.

As for MgO substrate, the deposited layer appears to be with the crystallographic PKN c-axis perpendicular to the substrate planar surface. This orientation within the film is characterized by the (00l) Bragg peaks of the PKN orthorhombic TTB structure. In Fig. 4a (MgO substrate) the (001) and (002) Bragg peaks of the PKN film are clearly visible, well separated from the substrate peaks. The latter (the (002) PKN peak) is at a somewhat higher 2θ value, above the (200) MgO peak. In the case of the STO substrate (Fig. 4b) the (100) line is still clearly present in the diffraction pattern though very close to the (100) STO peak, whereas the (200) PKN Bragg peak is not separated from the (200) STO peak; its presence can be deduced from the asymmetrical shape of the diffraction intensity occurring in the 2θ range between 46 and 47°.

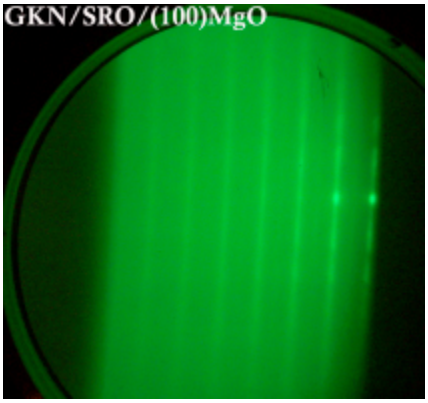

Fig. 5: RHEED image recorded with GKN deposited thin film on SRO/(100)MgO

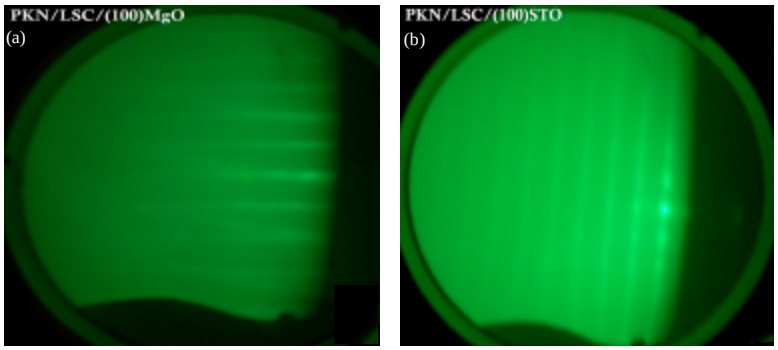

Fig. 6(a-b): RHEED image of (a) PKN/MgO thin film and (b) PKN/STO thin film

The crystalline quality of the thin films deposited on both substrates appears to be good, as shown from the Full Width at Half Maximum (FWHM) of the (00l) PKN Bragg peak that can be deduced from data, as compared to the values for the peak due to the substrate. The results show that the PKN film grown on the STO substrate has a better crystalline quality, compared to that grown on LSC/MgO substrate (FWHM is 0.206° for the (002) PKN/MgO and 0.153° for the (002)PKN/STO).

Electron diffraction (RHEED) and SEM results: The deposition chamber is equipped with a RHEED analyser to control epitaxial growth of the oxides. The RHEED pattern permits us to confirm the regular growth of the thin film with a smooth surface proved by the presence of straight lines in the RHEED images as shown in Fig. 5.

We present in Fig. 6, the RHEED patterns obtained with the PKN films deposited on MgO and STO substrates.

Again, these pictures exhibit the flatness of the surface of PKN thin films, characterised by the presence of the parallel lines without disorder. This confirms that there occurs a regular crystallographic structure and unit cell positions on the substrate, corresponding to a good quality epitaxial growth of the PKN film.

Figure 6b shows the RHEED pattern recorded on PKN thin film deposited on STO substrate. From the two patterns the presence of parallel lines indicates their epitaxial growth, with a

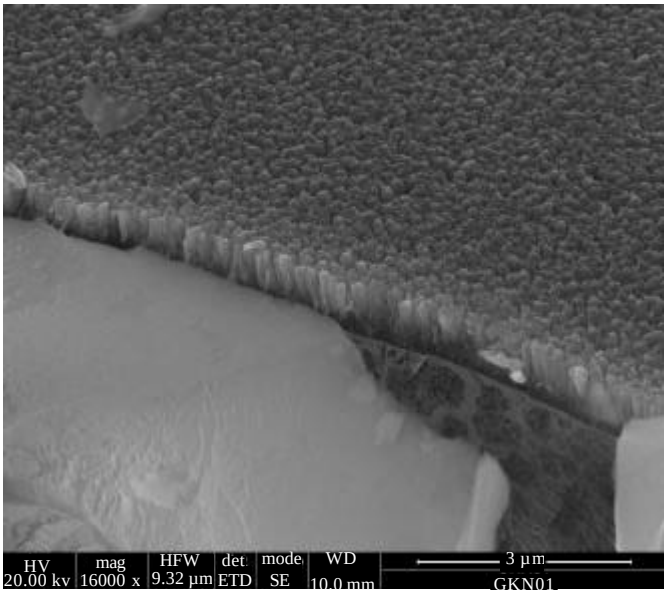

Fig. 7: SEM image of GKN thin film showing columnar ordering

particular high brightness on the PKN thin film grown on STO. Whatever the orientation of RHEED lines associated to the GKN/SRO/(100)STO and PKN/LSC/(100)MgO thin films in the direction perpendicular to the incident beam, they are unusual. Unit cells in these two cases seem to be turned in epitaxial reordering perpendicular to the incident beam. This situation can be attributed to preferential orientation of unit cells imposed by the substrates or the tetragonal structure in GKN.

To have complementary information on the structural organization of our layers, we performed observations using Scanning Electron Microscopy (SEM). Figure 7 shows the typical topography of the surface of a GKN thin film, with a homogenous distribution of the grains in its entire volume. This observation confirms the above results on the crystallization of GKN thin film. We can remark also the columnar growth as rods of GKN thin film perpendicular to the substrate.

CONCLUSION

Good quality GKN and PKN thin films have been obtained using Pulsed Laser Deposition (PLD) technique on SRO/(100) MgO substrate. We also obtained well crystallized PKN thin films on STO substrates. The deposited compounds remain in the same structure as that of bulk material : GKN in quadratic phase, PKN in its TTB orthorhombic structure. In all cases, thin films are oriented in c-axis direction and the structural organization as evidenced by RHEED is regular. Observation of the spatial arrangement in the case of GKN exhibits a regular columnar deposition.

More detailed studies are necessary to better understand the structural organization at different scales and physical properties, as the fatigue and damage processes in bulk (Bassiouny, 2005) and in thin film materials but it appears already that such layers may have important applications. Moreover, the systematic observed orientation with the crystalline c-axis perpendicular to the substrate layer, opens the possibility to elaborate well organized thin films with a multilayer structure, in which the chemical composition may vary along the c-axis, leading to the possibility of tailoring physical properties. This requires a better understanding of the defects present in the films, a work which is now in progress.

ACKNOWLEDGMENT

This work was supported by the Hubert Curien Volubilis project (MA/165) and by the Seventh Framework Programme (FP7) through the (IRSES-GA-2008-230832) project (ROBOCON).

REFERENCES

Aronson, L.B. and L. Hesselink, 1990. Photorefractive integrated-optical switch arrays in LiNbO3. Opt. Lett., 15: 30-32.

Bassiouny, E., 2005. Damage mechanics in ferroelectric ceramics-model and application. J. Applied Sci., 5: 257-266.

Castellans, R.N. and L.G. Feinstein, 1979. Ion-beam deposition of thin films of ferroelectric lead zirconate titanate (PZT). J. Applied Phys., 50: 4406-4411.

Hesselink, L. and M.C. Bashaw, 1993. Optical memories implemented with photorefractive media. Opt. Quantum Electron, 25: S611-S661.

Kimura, H., K. Maiwa, A. Miyazaki, K. Chinnavenkadasamy and Z. Cheng, 2005. Growth of lead potassium niobate crystal from melt. J. Cryst. Growth, 275: e833-e838.

Mohammadkhani, M., J. Fariborz and A.M. Kassai, 2010. Growth and characterization of p-type InSb on n-type (111) and (110) InSb substrates using molecular beam epitaxy. J. Applied Sci., 10: 1489-1491.

Rodriguez-Carvajal, J., 1993. Recent advances in magnetic structure determination by neutron powder diffraction. Physica B: Condensed Matter, 192: 55-69.

Sakamoto, S. and T. Yazaki, 1973. Longitudinal electro-optic effects in barium strontium niobate (BaxSr1_xNb2Og). J. Appl. Phys., 44: 254-262.

Tse, W.L. and W.L. Chan, 2003. A file system implementation for microcontroller using ferroelectric random access memory. Inform. Technol. J., 2: 52-57.

Vre, R.D. and L. Hesselink, 1994. Analysis of photorefractive stratified volume optical holographic optical elements. J. Opt. Soc. Am., B11: 1800-1808.

Webster, J.C. and F. Zernike, 1976. A sputtered optical waveguide amplitude modulator on a $LiNbO_3$ substrate. Ferroelectrics, 10: 249-251.

Zhang, Y.L., X.S. Xie, D. Mo, E.Y.B. Pun and L.P. Shi, 1996. Growth and photorefractive properties of Mn-doped (KNa)(0.1)(Sr0.6Ba0.4)(0.9)Nb_2O_6 crystals. J. Appl. Phys. (In Press).